

Optimization of resistive switching performance of metal-manganite oxide interfaces by a multipulse protocol

N. Ghenzi, M. J. Sánchez, M. J. Rozenberg, P. Stolar, F. G. Marlasca, D. Rubi, and P. Levy

Citation: *Journal of Applied Physics* **111**, 084512 (2012); doi: 10.1063/1.4705283

View online: <https://doi.org/10.1063/1.4705283>

View Table of Contents: <http://aip.scitation.org/toc/jap/111/8>

Published by the *American Institute of Physics*

Articles you may be interested in

[Understanding electroforming in bipolar resistive switching oxides](#)

Applied Physics Letters **98**, 042901 (2011); 10.1063/1.3537957

[Hysteresis switching loops in Ag-manganite memristive interfaces](#)

Journal of Applied Physics **107**, 093719 (2010); 10.1063/1.3372617

[Two resistive switching regimes in thin film manganite memory devices on silicon](#)

Applied Physics Letters **103**, 163506 (2013); 10.1063/1.4826484

[Tuning the resistive switching properties of TiO_{2-x} films](#)

Applied Physics Letters **106**, 123509 (2015); 10.1063/1.4916516

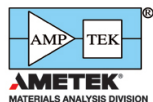
[Uniform resistive switching with a thin reactive metal interface layer in metal-La_{0.7}Ca_{0.3}MnO₃-metal heterostructures](#)

Applied Physics Letters **92**, 202102 (2008); 10.1063/1.2932148

[Resistive switching of rose bengal devices: A molecular effect?](#)

Journal of Applied Physics **100**, 094504 (2006); 10.1063/1.2364036

Ultra High Performance SDD Detectors



See all our XRF Solutions

Optimization of resistive switching performance of metal-manganite oxide interfaces by a multipulse protocol

N. Ghenzi,¹ M. J. Sánchez,² M. J. Rozenberg,^{3,4} P. Stoliar,^{1,5} F. G. Marlasca,¹ D. Rubi,^{1,5} and P. Levy¹

¹GIA, GAIANN-CAC—CNEA, Av. Gral Paz 1499 (1650) San Martín, Argentina

²Centro Atómico Bariloche and Instituto Balseiro, CNEA, (8400) San Carlos de Bariloche, Argentina

³Laboratoire de Physique des Solides, UMR8502 Université Paris-Sud, Orsay 91405, France

⁴Departamento de Física Juan José Giambiagi, FCEN, Universidad de Buenos Aires, Ciudad Universitaria Pabellón I, (1428) Buenos Aires, Argentina

⁵ECyT, Universidad Nacional de San Martín, Campus Miguelete, Martín de Irigoyen 3100 (1650) San Martín, Argentina

(Received 24 October 2011; accepted 10 March 2012; published online 30 April 2012)

We explore different resistance states of $\text{La}_{0.325}\text{Pr}_{0.300}\text{Ca}_{0.375}\text{MnO}_3$ – Ti interfaces as prototypes of non-volatile memory devices at room temperature. In addition to high and low resistance states accessible through bipolar pulsing with one pulse, higher resistance states can be obtained by repeatedly pulsing with a single polarity. The accumulative action of successive pulsing drives the resistance towards saturation, the time constant being a strong function of the pulsing amplitude. The experiments reveal that the pulsing amplitude and the number of applied pulses necessary to reach a target high resistance value appear to be in an exponential relationship, with a rate that results independent of the resistance value. Model simulations confirm these results and provide the oxygen vacancy profiles associated to the high resistance states obtained in the experiments. © 2012 American Institute of Physics. [<http://dx.doi.org/10.1063/1.4705283>]

I. INTRODUCTION

Metal-transition metal oxide (TMO) cells that exhibit resistive switching (RS) are prominent candidates for building blocks in non volatile memory applications.^{1,2} The transition from the high resistance state (HR) to the low resistance state (LR) is driven by a SET stimulus, while a RESET pulse settles the transition from the LR to the HR state. If the writing SET/RESET stimuli are of different polarities the RS is called bipolar, otherwise it is named unipolar RS.³

It is nowadays widely accepted that the redistribution of oxygen vacancies near the metal-oxide interface determines the main features of the bipolar RS response.^{2,3}

A recent model that succeeded in reproducing non trivial experimental findings of bipolar RS indicates that the migration of oxygen vacancies in a nanoscale vicinity of the metal-oxide interface is at the origin of the most significant resistive changes in complex TMO based cells. Our voltage-enhanced oxygen vacancy (VEOV) migration model⁴ assumes that the local resistivity is a function of the oxygen vacancy concentration and that the interfaces are highly resistive regions in which important electric fields, proportional to the current density and to the local resistivity, can be developed.

When a SET pulse is applied, the local electric field along the interfaces results strong enough to move the oxygen vacancies, changing its profile and hence the resistance of the device. After this initial redistribution of vacancies, a pulse with the opposite polarity (i.e., RESET) will not reproduce the previous profile of the electric field, preventing the device to return to the original resistance value after the completion of the pulsing cycle. The repetition of this process will produce a drift of the switching resistance levels

and the HR/LR ratio, which eventually fully degrades the memory performance. The redistribution of vacancies and related electric field profiles upon bipolar pulsing were recently analyzed in detail.⁵

The strategies reported in the literature to overcome the degradation problem are mainly based on the design of the device and the selection of materials.^{6–9} Strategies based on cancelling the drift using an asymmetric amplitude pulsing protocol were also shown to be successful.¹⁰ Following these ideas here, we propose as a possible strategy to optimize the performance of the device, a multipulse protocol that consist of applying pulses of a single polarity to a given HR state. We show, both through experiments and modelling, that in this case, the resistance evolves to (much) higher values than the initial HR state, increasing the HR/LR ratio, and thus the performance of the device as a memory cell. Our experimental results reveal that the number of pulses and required switching amplitude to reach a given HR state are related by an exponential relationship. We perform numerical simulations that, besides reproducing the experimental data remarkably well, enable a further study of the vacancy profiles associated to each resistance value, providing important confirmation for the theoretical assumptions of the model.

II. EXPERIMENTAL

Devices exhibiting RS were obtained using polycrystalline manganite $\text{La}_{0.325}\text{Pr}_{0.300}\text{Ca}_{0.375}\text{MnO}_3$ (LPCMO) with Ti contacts. The devices were fabricated on top of a 1 mm-thick sintered LPCMO sample. The 500 nm-thick, 500 μm diameter metal pads were sputtered through a shadow mask. The nearest distance between pads is approximately 1 mm. The electrical characterization was performed with a Source

Meter Unit (SMU) Keithley 2400. The SMU applies the writing and reading pulses through the A and C pads and measures the voltage drop between the B and C contacts in order to evaluate the resistance of the C interface.¹¹

Initially, to induce RS on the virgin sample, a forming procedure as described in Ref. 12 was followed. RS was then obtained by applying pulses of the same amplitude and opposite polarity (write operation). Each writing pulse of 10 ms time width was followed by a small bias I_b applied 1 s after the writing pulse, to obtain the remnant resistance (read operation).

III. RESULTS AND DISCUSSION

Figure 1(a) depicts the resistance values $R = V_{BC}/I_b$ for the right C interface (close to electrode C) as a function of the number of pulses. We begin the pulsing protocol by performing alternating polarity pulses of $I_p = 200$ mA during the first 500 pulses. As observed, the resistance R exhibits two states with values that decrease smoothly and monotonically from the initial HR and LR states, as a signature of the aforemen-

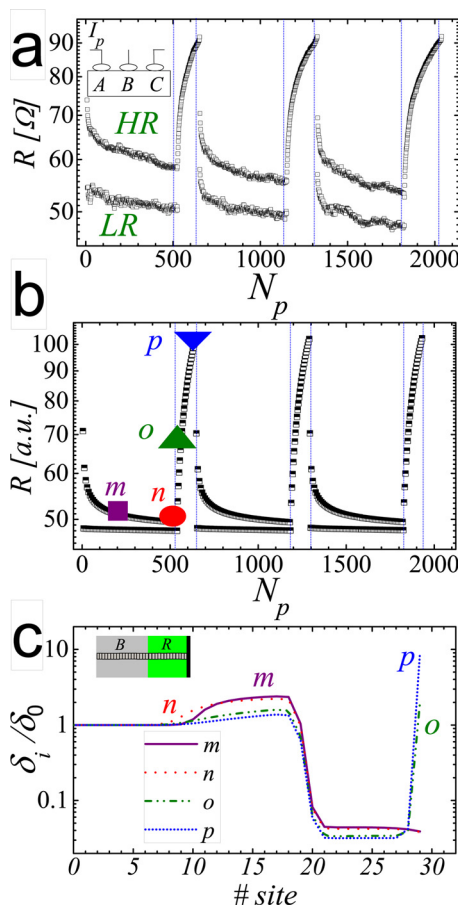


FIG. 1. (a) Three cycles consisting of alternating polarity pulsing (initial 500 pulses) followed by single positive polarity (RESET) pulsing (next 125 pulses), using $I_p = 200$ mA for a Ti-LPCMO interface at room temperature. Resistance values were measured by means of a small I_b current. Inset: scheme of the experimental set up. (b) Simulation of the same pulsing protocol for a stimulus $I_p^s = 150$ a.u. (c) Simulated density vacancy profiles δ_i/δ_0 at site i for selected states labeled m, n, o, p in (b). Sites 0–20 correspond to the bulk (B) and sites 21–30 to the right interface (R). Inset: scheme of bulk-interface region employed in the simulations. Otherwise stated, model parameters are as in Ref. 4 that it can be seen for further details.

tioned degradation process. After the first sequence of pulses, a second one, consisting of positive (RESET) pulses of the same amplitude, was applied. This leads the HR state to evolve into states of higher resistances, reaching around 90Ω after 125 pulses, with a tendency towards saturation.

When the alternating pulsing was reinitiated at $N_p = 625$, the initial HR and LR states were recovered, although we got a slightly larger value for the LR and a smaller one for the HR, respectively. As the pulsing sequence was repeated, a similar trend was obtained, as shown in Fig. 1(a). However, as a consequence of the degradation process and of the slightly different initial HR and LR values, the following sequence of positive pulses requires a larger amount of pulsing events to reach a predetermined target for the HR value (i.e., 90Ω in Fig. 1(a)).

The above described pulsing protocol was simulated using the VEOV migration model introduced in Ref. 4. As shown in Fig. 1(b), main experimental features were captured by the simulation. Figure 1(c) depicts the vacancy density profile in the neighbourhood of the simulated bulk(B)-right(R) interface along selected resistance states.

The oxygen vacancies migration is enhanced at the oxide-metal interfacial regions, with the ions moving either towards the electrode or the bulk, depending on the polarity of the applied stimulus. For instance, a positive (RESET) pulse applied on A will push vacancies from the bulk to the C interface (right(R) interface in the simulations), while a negative (SET) one produces the migration of vacancies from the C interface towards the bulk.

The effect of successive SET/RESET pulses is described as follows. Starting from a HR state, vacancies migrate from the right interface towards the bulk under a SET pulse. At the bulk, the drift of vacancies virtually stops, since at that region the electric field is much smaller than at the interface. A RESET pulse of the same intensity than the former applied SET cannot reinject the original amount of vacancies at the right interface, preventing the same value of the original HR state. Successive cycles yield a cumulative effect, with a depletion of vacancies at the right interface and an accumulation at the bulk side of the interface-bulk boundary (see profile m in Fig. 1(c)). Thus, for alternating pulsing polarity, the monotonous decrease of the initial HR and LR states corresponds to a net drift process in which vacancies migrate from the right interface towards the bulk region. A detailed description of this process was given in Ref. 5.

On the other hand, for the sequence of successive RESET pulses, i.e., pulses with non alternating polarity, vacancies tend to pile up at the right end of the right interface in an accumulative process, with a concomitant increase of the resistance above the initial HR value. As expected, in this case, the concentration of vacancies at the bulk gradually decreases, exhibiting a tendency towards saturation for larger number of pulses. This is clearly observed in the vacancy profiles of Fig. 1(c) associated to the highest HR values, points o and p , respectively, in Fig. 1(b).

We have also tested that the LR state is much less susceptible to the accumulation of negative pulses. As its resistance is lower than the HR one, the associated electric fields are smaller, producing less pronounced effects.

With the aim of reaching higher HR values, a practical question that emerges is whether it is a better strategy to increase the amplitude of the pulses or to accumulate pulses having the same electrical stress.

To further characterize the accumulation of vacancies at the different high resistance states obtained upon pulsing with a single polarity, additional measurements were performed by varying the pulsing stimulus I_p . The accumulation protocol always starts from a similar HR initial state, R_0 , the one obtained after inducing bipolar RS several times. Fig. 2(a) depicts the obtained resistance values as a function of the number of RESET pulses N_p , for increasing amplitudes ranging from 200 to 400 mA. Data were normalized to the corresponding initial resistance value R_0 to allow comparison. All the amplitudes tested exhibit a monotonous growth of the resistance as the number of applied pulses increases. Note that a tendency towards saturation in the high resistance values is observed, it being more evident for the lower amplitudes. For increasing pulsing amplitudes, higher resistance values were obtained. This is shown in the inset of Fig. 2(a) for $N_p = 650$, where the increase of the HR values with I_p follows an exponential dependence. In addition, the amount of pulses required to reach a certain value R/R_0 appears to be inversely proportional to the pulsing amplitude (see Fig. 3 and discussion below).

The correspondent simulations, plotted by solid lines, appear to be in excellent agreement with the experimental

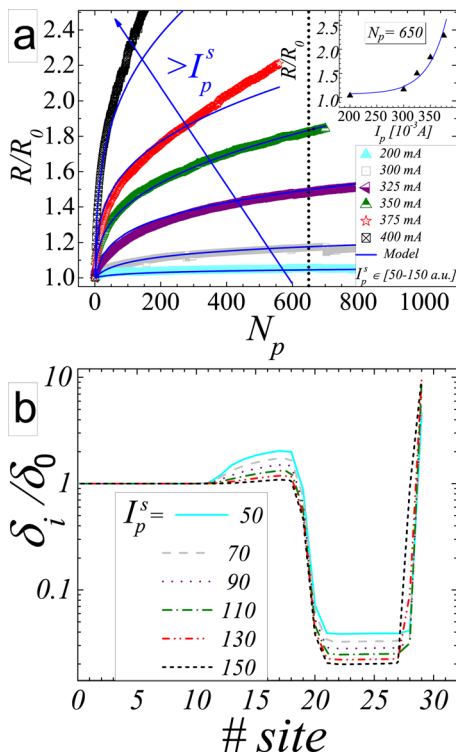


FIG. 2. (a) Normalized HR resistance values of a Ti-LPCMO interface obtained upon pulsing with single polarity RESET pulses of different amplitudes, starting from an initial R_0 value. Model simulations are also shown by the blue solid lines. The arrow indicates the direction of increasing amplitudes. Inset: Experimental values R/R_0 vs. pulsing amplitude for $N_p = 650$ (vertical line in a). The solid line is an exponential fit. (b) Simulated vacancies density profiles δ_i/δ_0 for selected $N_p = 650$ pulses and different simulated stimulus amplitudes in the range $I_p^s = 50 - 150$ a.u.

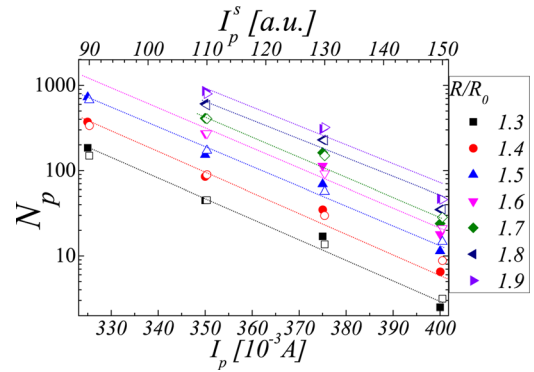


FIG. 3. Semilog plot of the number of pulses N_p vs the experimental (simulated) stimulus pulsing $I_p(I_p^s)$ for different values R/R_0 selected from Fig. 2. Solid (open) symbols correspond to experimental (simulated) data.

results. The different high resistance values attained for increasing stimuli can be correlated with the associated vacancy profiles. For a selected number of pulses ($N_p = 650$), Fig. 2(b) shows that the vacancy density profile δ_i at the bulk side closer to the right interface tends to flatten, reaching for larger pulsing amplitudes an almost uniform distribution with attained values quite undistinguishable from the bulk ones. In correspondence, the vacancies at the right interface exhibit a remarkable accumulation close to the right electrode.

As both experiments and simulations show, higher resistance states can be obtained either by increasing the pulsing amplitude, or by insisting on accumulating pulses. Therefore a given high resistance state can be reached for different combinations of (I_p, N_p) values. Overall results suggest that (I_p, N_p) have an exponential dependence, i.e., $N_p \propto \exp(-I_p/\alpha)$, with the parameter α almost independent of the R/R_0 ratio. This finding is explicitly shown in Fig. 3. It was constructed by determining the amount of pulses N_p required, for each pulsing amplitude I_p , to reach a certain (normalized) resistance value R/R_0 . As shown, experimental data can be reasonably fitted by an exponential dependence with $\alpha \sim 20$ mA. Moreover, note that the simulated data follows remarkably well the experimental results.

Our voltage-enhanced oxygen vacancy (VEOV) migration model provides a transparent picture of our experimental results. Details on the VEOV model and its associated equations are given in Refs. 4 and 10.

The crucial insights are: (i) as vacancies move across the boundary between the bulk region into the interfacial region (that is across sites 18 – 21 in our simulation data of Fig. 1(c) and 2(b)), their contribution to the change in the total resistance is significantly increased. From the VEOV model, we have $\delta_{int}^{tot} \propto \Delta R$, i.e., the increase in resistance is directly given by the increase in the total number of vacancies entering the interfacial region. (ii) The probability to jump from the bulk to the interface during a single pulse I_p is $\propto \exp(e\Delta V/kT)$, where ΔV is the local voltage drop (e is the electron charge), and $\Delta V \propto I_p \delta_{bdy}$, where δ_{bdy} is the (mean) density of vacancies at (bulk side of) the boundary, which remains $\delta_{bdy} \approx \delta_0$.

From (i) and (ii), we have that the cumulative change of resistance after the application of N_p consecutive positive (RESET) pulses can be simply described by

$$\Delta R \sim N_p \exp(cI_p), \quad (1)$$

where c is a constant that has units of inverse current. The above expression describes well the exponential increase of the high resistance (notice that $\Delta R = R - R_0 = R_0(R/R_0 - 1)$), with the intensity of the applied current for a fixed number of applied pulses, which is shown in the inset of Fig. 2(a) for $N_p = 650$. In addition, taking the logarithm on both sides, we get (up to an unimportant overall constant), $\ln(N_p) = -cI_p + \ln(\Delta R)$, which explains the experimental data of Fig. 3. In fact, it predicts (1) the linear relation between $\ln(N)$ and the intensity of the applied current I_p , (2) an y-ordinate given by ΔR , and (3) a slope given by the constant c .

Moreover, one may argue, from insight (ii), that the constant c should depend inversely on the temperature (as mentioned we got $1/c = \alpha \sim 20$ mA from experimental data at room temperature). Whether this is the case or if the temperature has an additional role in the switching effect, as argued in Ref. 13 (see also Refs. 2 and 14), is an important issue left for future study.

For a given stimulus amplitude, the N_p variable could be associated to the timewidth of an effective single pulse, meaning that several pulses should have the same effect as a longer one. Hence, Fig. 3 suggests that our data (both experiments and simulations) would follow an exponential stimulus-timewidth dependence.

Exponential voltage-timewidth relationships were previously observed in binary oxide based memory cells such as ZnO,¹⁵ TaO,¹⁶ and HfO/AIO.¹⁷ The origin of the switching dynamics was attributed to ion hopping processes assisted by Joule heating through the potential wells of the oxide matrix.¹⁸ Here, we have explicitly shown that for Ti-LPCMO interfaces the local electric field enhanced redistribution of oxygen vacancies is responsible for the observed universal switching dynamics.

In Ref. 2, it was suggested that the switching mechanism should involve a strong nonlinearity in the electric field dependence. This is explicitly contained in our VEOV model through the vacancy hopping probability $\propto \exp(e\Delta V/kT)$.^{4,5}

Upon bipolar pulsing, the transition from LR to HR proceeds through the gradual migration of vacancies from the bulk to the whole interfacial layer, in a rather homogeneous way.⁵ On the contrary, as the accumulative pulsing onto the HR state produces a large accumulation of vacancies in a region near the electrode (modeled by the last 10 sites in Figs. 1(c) and 2(b), the resistivity there will experience a significant increase (it is proportional to the vacancy concentration). The large local resistivity leads to a very large local electric field that upon inverting the pulse polarity will immediately drive the accumulated vacancies out of the electrode region and back into the bulk.

Thus, our VEOV migration model also provides insights on the origin of the dramatic decrease of resistance due to a single SET pulse applied after a RESET pulsing train. Based on this finding, we propose as a strategy to increase the HR/LR ratio to have an unbalanced pulsing, consisting of $N+$ successive RESET pulses pushing vacancies gradually into the interface, and a single SET pulse releasing all the

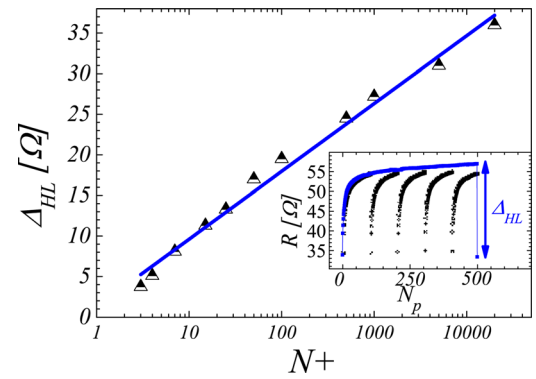


FIG. 4. Resistance change $\Delta_{HL} \equiv HR - LR$ as a function of the number of $N+$ pulses followed by a single SET pulse, always using $I_p = 200$ mA. The line is a guide for the eye. Inset: Raw data comparing five consecutive runs with $N+ = 100$ (black circles) with data of one run with $N+ = 500$ (blue squares).

accumulated vacancies in one step. In this way, using $N+ = 10, 100, 1000$ and $10\,000$, with $I_p = 200$ mA, we obtained $\Delta_{HL} \equiv HR - LR = 9.6, 18, 26.4,$ and 35 Ω , suggesting a slow but clear tendency towards an enhanced response, as shown in Fig. 4.

In summary, we have proposed a multipulse protocol that allows the study of resistive switching dynamics in a Ti-LPCMO interface upon sequential application of single polarity pulses. Based on the VEOV migration model,⁴ the scaling dependence $\Delta R \propto N_p \exp(I_p c)$ is demonstrated. This simple physical relationship reveals that, to achieve a given high resistance target state (a higher HR/LR ratio), it is more efficient to increase the pulse amplitude rather than to accumulate pulses of a given amplitude. The agreement of overall experimental data with simulations validates the proposed model assumptions and its associated equations. Thus, an unbalanced number of SET/RESET pulses is demonstrated to be a plausible strategy to optimize the actual response of a device.

ACKNOWLEDGMENTS

We acknowledge financial support from CNEA, CONICET (PIP11220080101821 and PIP047-2008), DuPont-CONICET, ANPCyT (PICT2006-483), Fundación Balseiro and UNSAM. M.J.S., M.J.R., D.R., and P.L. are fellows of CONICET.

¹D. B. Strukov, G. S. Snider, D. R. Stewart, and R. S. Williams, *Nature* **453**(, 80 (2008).

²R. Waser, R. Dittmann, G. Staikov, and K. Szot, *Adv. Mater.* **21**, 2632 (2009).

³M. Rozenberg, *Scholarpedia* **6**(4), 11414 (2011).

⁴M. Rozenberg, M. J. Sánchez, R. Weht, C. Acha, F. G. Marlasca, and P. Levy, *Phys. Rev. B* **81**, 115101 (2010).

⁵N. Ghenzi, M. J. Sánchez, F. Gomez-Marlasca, P. Levy, and M. J. Rozenberg, *J. App. Phys.* **107**, 093719 (2010).

⁶W. Shen, R. Dittmann, U. Breuer, and R. Waser, *Appl. Phys. Lett.* **93**, 222102 (2008).

⁷M. K. Yang, J.-W. Park, T. K. Ko, and J.-K. Lee, *Appl. Phys. Lett.* **95**, 042105 (2009).

⁸D. S. Shang, L. Shi, J. R. Sun, B. G. Shen, F. Zhuge, R. W. Li, and Y. G. Zhao, *Appl. Phys. Lett.* **96**, 072103 (2010).

⁹R. Yang, X. M. Li, W. D. Yu, X. D. Gao, D. S. Shang, and L. D. Chen, *J. Appl. Phys.* **107**, 063703 (2010).

¹⁰F. Gomez-Marlasca, N. Ghenzi, P. Stoliar, M. J. Sánchez, M. J. Rozenberg, G. Leyva, and P. Levy, *Appl. Phys. Lett.* **98**, 123502 (2011).

- ¹¹M. Quintero, P. Levy, A. G. Leyva, and M. J. Rozenberg, *Phys. Rev. Lett.* **98**, 116601 (2007).
- ¹²F. Gomez-Marlasca, N. Ghenzi, M. J. Rozenberg, and P. Levy, *App. Phys. Lett.* **98**, 42901 (2011).
- ¹³S. Menzel, M. Waters, A. Marchewka, U. Böttger, R. Dittmann, and R. Waser, *Adv. Funct. Mater.* **21**, 4487 (2011).
- ¹⁴M. Janousch, G. Meijer, U. Staub, B. Delley, S. Karg, and B. Andreasson, *Adv. Mater.* **19**, 2232 (2007).
- ¹⁵B. Gao, S. Yu, N. Xu, L. F. Liu, B. Sun, X. Y. Liu, R. Q. Han, J. F. Kang, B. Yu, and Y. Y. Wang, *Tech. Dig. - Int. Electron Devices Meet.* **2008**, 53.
- ¹⁶T. Tsuruoka, K. Terabe, T. Hasegawa, and M. Aono, *Nanotechnology* **21**, 425205, (2010).
- ¹⁷S. Yu, Y. Wu, and H.-S. Philip Wong, *Appl. Phys. Lett.* **98**, 103514 (2011).
- ¹⁸N. F. Mott and R. W. Gurney, *Electronic Processes in Ionic Crystals* (Clarendon, Oxford, 1948).